

Analysing Laser Machined YBCO Microbridges Using Raman Spectroscopy and Transport Measurements Aiming to Investigate Process Induced Degradation

K. LANGE¹, M. SPARKES^{1,*}, J. BULMER², J.P.F. FEIGHAN², W. O'NEILL¹ AND T.J. HAUGAN³

¹*Institute for Manufacturing, 17 Charles Babbage Road, University of Cambridge, Cambridge, CB3 0FS, UK.*

²*Department of Materials Science & Metallurgy, 17 Charles Babbage Road, University of Cambridge, Cambridge, CB3 0FS, UK.*

³*AFRL/RQQM, US Air Force Research Laboratory, Wright-Patterson AFB, OH 45433-0000, USA.*

Machining high temperature superconducting (HTS) thin films is challenging due to the material's sensitivity. Here, 200 nm thick YBCO microbridges were machined with a femtosecond laser (300 fs at 1030 nm wavelength) as a chemical free and flexible method with minimal edge damage. Transport measurements and Raman spectroscopy were used to analyse the bridges before and after laser processing. While transport and Raman measurements are commonly used separately to evaluate YBCO, our approach links both techniques to analyse laser induced damage. The link between changes in the Raman spectrum and transport measurements is investigated by identifying changes caused by repeated heat treatments while sequentially measuring the critical current density and Raman spectra. The data obtained is used to predict critical current density losses from changes in Raman peak intensities and shifts. This technique is further investigated by applying it to laser machined YBCO bridges which were exposed to highly localised heating. Results show that for bridge widths of 10 μm , a femtosecond laser can be used to repeatedly successfully machine microbridges with no loss in critical current density and that there is some correlation to critical current changes in the Raman spectra.

Keywords: Femtosecond laser, $\text{YBa}_2\text{Cu}_3\text{O}_{7-x}$ micromachining, thin films, heat treatments, transport measurements, Raman spectroscopy

*Corresponding author: E-mail: mrs46@cam.ac.uk

1 INTRODUCTION

Since their discovery, high temperature superconductors (HTS) have been used in various applications such as microwave filters, antennas, single photon bolometers and more [1, 2]. The most researched HTS is $\text{YBa}_2\text{Cu}_3\text{O}_{7-x}$ due to its high critical temperature (<90 K). Most applications require patterning of YBCO on a micro/nanoscale; however, this proves to be very challenging due to the material's sensitivity, since the superconductivity is easily lost by heat degradation, chemical interaction, electron/ion irradiation and humidity [3-6].

Current machining techniques are lithography (wet and dry) [7, 8], Focused ion beam (FIB) [9, 10] and laser machining ($>$ fs) [9]. While lithography is comparably quick, it does not allow much design freedom as a new mask would be required for each design change. Another disadvantage is the degrading effect on YBCO caused by chemicals and/or electron beams used in lithography. FIB machining has a high design resolution and flexibility as the design can be easily changed using computer-aided design (CAD) software, with helium FIBs achieving nanometre feature sizes [10]. FIBs have two major disadvantages: one being the very limited processing speed; and the other being ion implantations which alter the crystal structure of YBCO leading to degradation. While laser machining offers the advantages of design flexibility and high processing speed, the challenge of controlling heat input requires consideration.

For this work a femtosecond laser was used operating at a wavelength of 1030 nm and a pulse width of 300 fs to machine YBCO microbridges to different widths. The laser gives limited thermal effects due to direct solid-vapour transitions. To evaluate the effects of the laser on YBCO, transport and Raman measurements were conducted. While transport measurement is the most common technique to evaluate HTS, Raman spectroscopy is added as a quick and non-contact measurement procedure to assess thermal damage which result in oxygen diffusion. Depending on the oxygen content of YBCO, the vibrational modes and their respective Raman peaks of the different atoms change [11, 12]. Since laser machining has several variables that could influence the Raman spectrum, YBCO thin films were also heated and measured as a reference.

2 EXPERIMENTAL PROCEDURES

YBCO (M-type) films of 200 nm thickness were grown on MgO substrate in a bridge arrangement (STAR Cryoelectronics LLC). Individual samples were composed of five bridges with 20 nm thick gold contacts, as can be seen in Figure 1. Heat treatments were conducted at room temperature in air. A heat plate was set to a temperature of 300°C and the sample heated for 10 seconds.

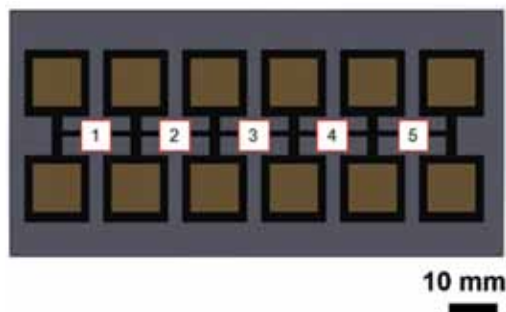


FIGURE 1
Schematic diagram of one YBCO sample with 5 bridges (numbered).

Laser machining was carried out with a femtosecond laser (SATSUMA; Amplitude Systèmes SA) emitting a Gaussian beam and operating at a wavelength of 1030 nm and pulse width of 300 fs in the manner shown in Figure 2. The YBCO bridges were processed under ambient conditions with the laser parameters listed in Table 1. The sample was mounted on a computer numerical control (CNC) stage which has an accuracy of $\pm 3 \mu\text{m}$ in the x - y -direction and $\pm 0.5 \mu\text{m}$ in the z -direction. To correct tip/tilt an additional stage was mounted onto the CNC stage. An objective lens (12OI09; COMAR Optics, Ltd.) of $\text{NA}=0.35$ with a focal length of 12.7 mm focussed the laser beam to a theoretical $1/e^2$ spot diameter of $4.58 \mu\text{m}$. To improve the machining edge quality a

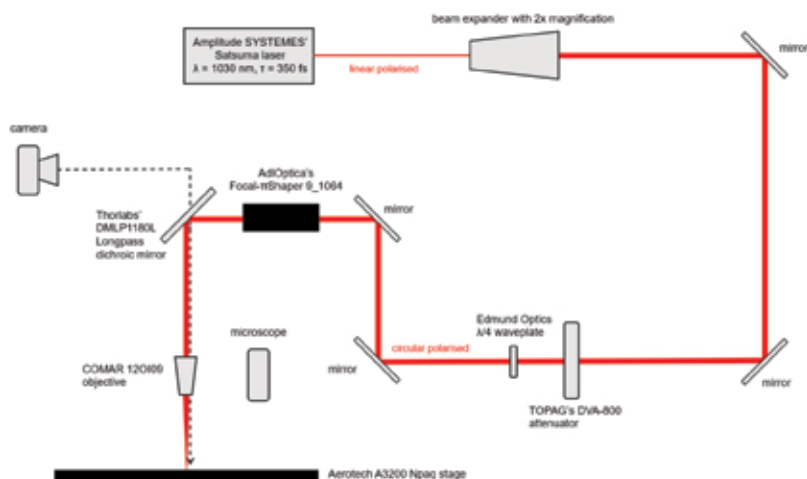


FIGURE 2
Schematic diagram showing the experimental configuration of the laser platform.

TABLE 1
Femtosecond laser specification.

Wavelength	1030 nm
Pulse duration	300 fs
Pulse repetition rate	1 to 2000 kHz
Raw beam diameter	2.0 ± 0.5 mm
M ²	1.1

beam shaper (Focal- π Shaper 9_1064; AdlOptica Optical Systems, GmbH) was added to the configuration to change the Gaussian beam profile to a flat top.

The transport and Raman properties of the YBCO samples were measured before and after heat/laser experiments with a Raman microscope (Senterra; Bruker Corporation) with an excitation wavelength of 532 nm and a 20 \times objective. At 532 nm the optical penetration depth of YBCO is 70 to 80 nm [13], approaching half the film thickness. The measurements were taken with 5 mW laser power over 10 seconds with three acquisitions over one data point with a spot size of <4 μ m.

3 RESULTS AND DISCUSSION

3.1 Laser ablation

After processing YBCO thin films with a range of pulse energies (36.7 nJ to 282 nJ), repetition rates and processing speeds, a pulse energy of 215 nJ at 1 kHz was determined to be optimum to machine YBCO bridges in one pass at 1 mm/s while avoiding damage to the MgO substrate. The bridges were machined from one side only including a 50 μ m radius to avoid current crowding. A comparison between the edges made by lithography and laser machining is shown in Figure 3. The RMS edge roughness for the lithography edge is 0.955 μ m with a peak-to-peak roughness of 3.43 μ m. The RMS edge roughness of the laser-processed sample is comparable to the lithography value of 0.957 μ m. The peak-to-peak value is slightly higher at 4.19 μ m.

3.2 Transport measurements

A four-point probe cooled in liquid nitrogen was used for the transport measurements. Spring-loaded pogo pins were connected to the gold pads using indium to increase the contact area. Current pulses from a source meter (2440; Keithley) were sent through the sample while the voltage was measured by a nanovoltmeter (2182; Keithley). To determine the critical current a criterion voltage of 0.5 μ V was used. During the heat treatments a 10 μ m

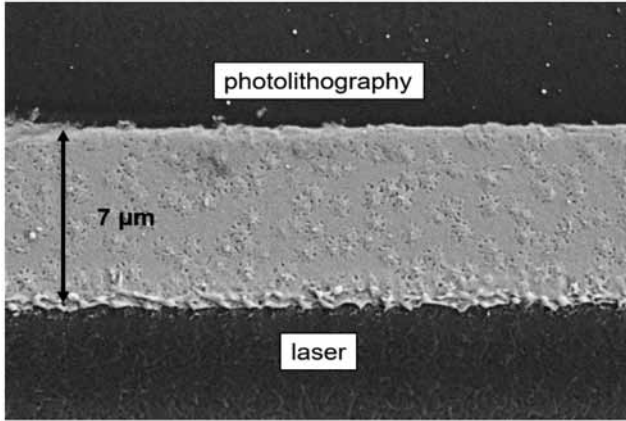


FIGURE 3
SEM micrograph of a 30 μm YBCO bridge machined to 7 μm. Both the photolithography and the laser edge are visible.

YBCO bridge sample was repeatedly measured. The decline of the critical current with each heat treatment, 10 seconds at 300°C, is shown in Figure 4.

3.3 Raman spectroscopy

As stated in the work of Li *et al.*[13], once YBCO has been degraded the Cu₂ peak intensity surpasses the Ba peak as a result of oxygen loss during the

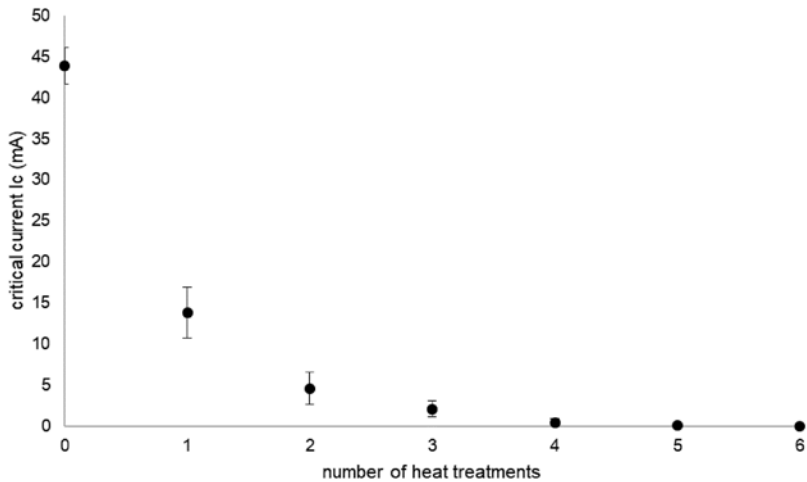


FIGURE 4
Graph showing the critical current decrease over multiple heat treatments of a 10 μm YBCO bridge sample. The error for the critical current is 140 μA at a criterion voltage of 0.5 μV.

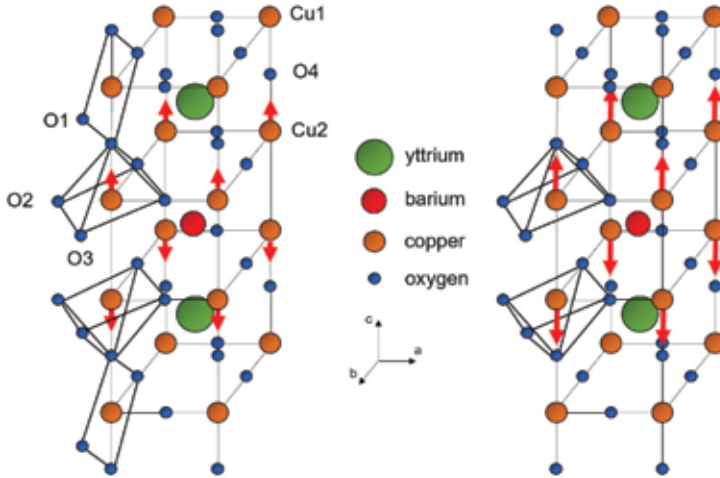


FIGURE 5

Crystalline structure of YBCO. The schematic on the left shows the orthorhombic structure of YBCO (superconducting) while on the right the tetragonal structure (insulating) is shown. The red arrows are indicating the Cu2 vibrational mode which is detected by Raman spectroscopy. The direction of the vibrational modes is further explained by Venkataraman *et al.* [14].

phase transition from the orthorhombic (superconducting) to the tetragonal (insulating) crystalline structure of YBCO, see Figure 5. In this study the Raman peak intensity change during the heat treatments was further analysed by relating Ba/Cu2 ratios to transport measurement results (see Figure 6 and Figure 7). With the decline of the Ba/Cu2 ratio, the critical current of the sample also decreased. Based on repeated heat treatment experiments, it appears that for this work, below a Ba/Cu2 ratio of 1.15, the YBCO sample is more likely to have lost its superconductivity.

Laser machined bridges were also examined using Raman to identify laser induced damage and possible heat influences. Spectra from laser machined bridges are shown in Figure 8. Bridge 1 was machined from 100 to 30 μm and the Raman spectra show slight changes in the peak intensities, especially a decrease in Ba. The width of Bridge 2 was reduced from 100 to 10 μm and the Raman spectra show a significant change in the Ba/Cu2 ratio, similar to the changes observed during the heat treatments. This suggests that the sample has degraded, confirmed by transport measurements. More laser machined bridges were inspected with Raman spectroscopy to investigate whether these spectral changes are repeatable (see Figure 9). The Raman intensity for both bridges changed after the laser process. The Ba/Cu2 ratio decreased from 1.25 to 1.18 for Bridge 3 (4% critical current density decrease) and from 1.27 to 1.18 for Bridge 4 (12% critical current density decrease). Similar to the heat treatment results, the Ba/Cu2 ratio decreased with decreasing current

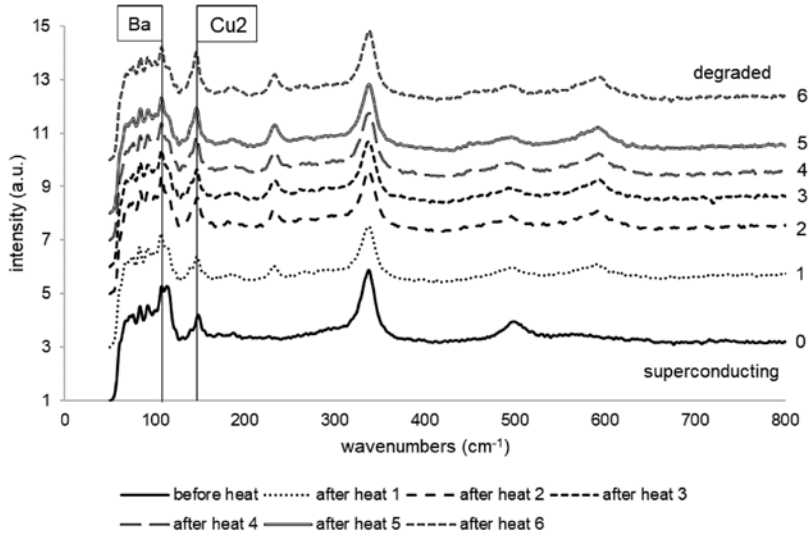


FIGURE 6 Changes in the Raman spectra are observed as the sample changes from superconducting to complete degradation. The different spectra are displayed with an offset for better distinction of the changes.

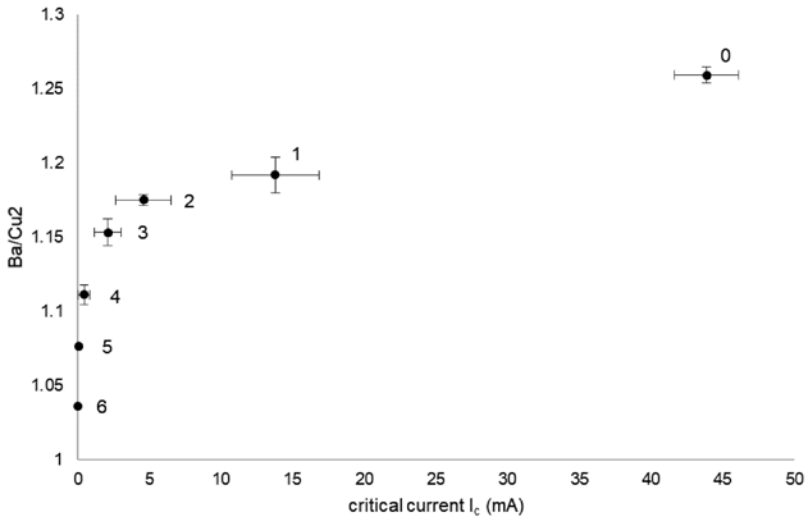


FIGURE 7 Graph showing the Ba/Cu₂ ratio *versus* critical current measured before and after heat treatments.

density. Yet, during the heat treatments, a Ba/Cu₂ ratio of 1.18 already showed an 83% critical current density decrease compared to a critical current density decrease of 4% to 12% when using the laser.

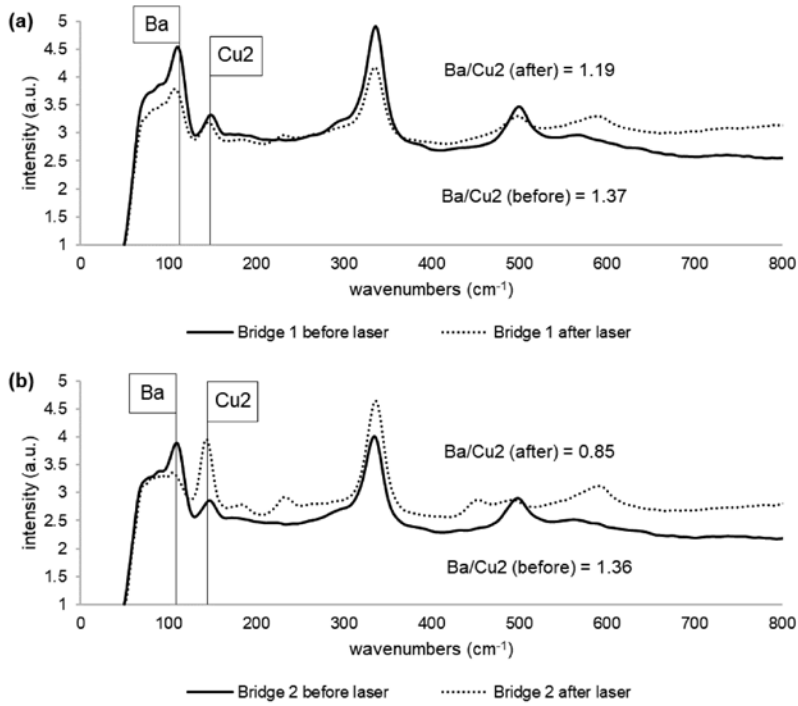


FIGURE 8 Raman spectra before and after the laser machining of (a) Bridge 1 and (b) Bridge 2.

Laser machining is a far more complex process than the heat treatments. These results let us assume that the Ba/Cu₂ ratio can give us some information about the state of a bridge after the laser process and that the bridges seem to have suffered from only limited heat effects. Defects (structural) might also play another role in terms of possible degradation sources.

4 CONCLUSIONS

A link between Raman spectroscopy and transport measurements was investigated. A decreasing Ba/Cu₂ ratio indicates a decreasing current density. With this ratio, Raman spectroscopy could have the potential to be used as a new inline measurement method to monitor the degradation of YBCO bridges. Comparing the results from heat treatments and femtosecond laser machining, similarities between Ba/Cu₂ ratios and critical current density were observed. The laser process introduces more variables that could be a degradation source than simple heat treatments. Raman measurements for laser

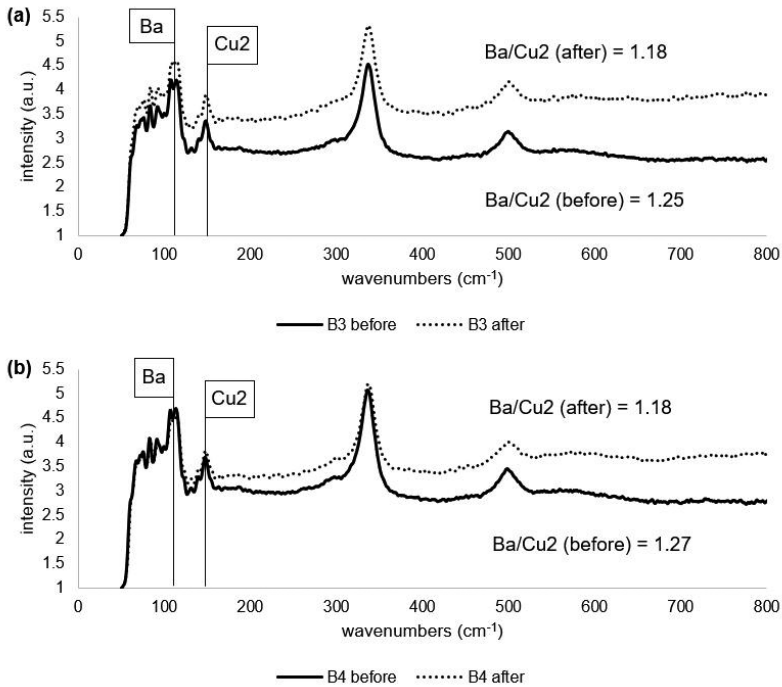


FIGURE 9

Raman spectra of (a) Bridge 3 when machined from 30 to 15 μm and (b) Bridge 4 from 30 to 6.8 μm at 1 kHz with a processing speed of 1 mm/s.

machined samples are also limited by the Raman spot size and the position accuracy of the respective sample stage.

ACKNOWLEDGEMENTS

This work was partially supported by the Air Force Research Laboratory - Aerospace Systems Directorate (AFRL/RQ), the Air Force Office of Scientific Research (AFOSR) under contract LRIR #18RQCOR100, and AFOSR/EOARD under contract FA 16IOE050 and the EPSRC EPSRC (Grant No. L016567/1).

REFERENCES

- [1] Aghabagheri S., Rasti M., Mohammadzadeh M.R., Kameli P., Salamati H., Mohammadpour-Aghdam K. and Faraji-Dana R. High temperature superconducting YBCO microwave filters. *Physica C: Superconductivity and its Applications* **549** (2018), 22–26.

- [2] Curtz N., Koller E., Zbinden H., Decroux M., Antognazza L., Fisher Ø. and Gisin N. Patterning of ultrathin YBCO nanowires using a new focused-ion-beam process. *Superconductor Science and Technology* **23**(4) (2010), 045015.
- [3] Nawaz S., Arpaia R., Lombardi F. and Bauch, T. Microwave response of superconducting $\text{YBa}_2\text{Cu}_3\text{O}_{7-\delta}$ nanowire bridges sustaining the critical depairing current: Evidence of Josephson-like behavior. *Physical Review Letters* **110** (2013), 167004.
- [4] Quere Y. (1989). *Irradiation damage in superconductors*. Retrieved 10th January 2018, from http://inis.iaea.org/Search/search.aspx?orig_q=RN:21039530.
- [5] Ballentine P.H., Kadin A.M., Fisher M.A., Mallory D.S. and Donaldson W.R. Microlithography of high-temperature superconducting films: Laser ablation vs. wet etching. *IEEE Transactions on Magnetics* **25**(2) (1989), 950-953.
- [6] Arpaia R., Nawaz S., Lombardi F. and Bauch, T. Improved nanopatterning for YBCO nanowires approaching the depairing current. *IEEE Transactions on Applied Superconductivity* **23** (2013), 1101505.
- [7] Lee S-G., Oh S-H., Kan C.S. and Kim S-J. Superconducting nanobridge made from $\text{YBa}_2\text{Cu}_3\text{O}_7$ film by using focused ion beam. *Physica C: Superconductivity* **460-462**, (2007), 1468-1469.
- [8] Wu C.H., Jhan F.J., Chen J.H. and Jeng J.T. High-Tc Josephson junctions fabricated by focused ion beam direct milling. *Superconductor Science and Technology* **26**(2) (2013), 025010.
- [9] Hix K.E., Rendina M.C., Blackshire J.L. and Levin G.A. (2004). *Laser micromachining of coated $\text{YBa}_2\text{Cu}_3\text{O}_{6+x}$ superconducting thin films*. Retrieved 18th October 2016, from <http://arxiv.org/abs/cond-mat/0406311>.
- [10] Cybart S.A., Cho E.Y., Wong T.J., Wehlin B.H., Ma M.K., Huynh C. and Dynes R.C. Nano Josephson superconducting tunnel junctions in $\text{YBa}_2\text{Cu}_3\text{O}_{7-\delta}$ directly patterned with a focused helium ion beam. *Nature Nanotechnology* **10** (2015), 598-602.
- [11] Maroni V.A., Reeves J.L. and Schwab G. On-line characterization of YBCO coated conductors using Raman spectroscopy methods. *Applied Spectroscopy* **61**(4) (2007), 359-366.
- [12] Iliev M.N., Hadjiev V.G. and Ivanov V.G. Raman spectroscopy of local structure and reordering processes in $\text{YBa}_2\text{Cu}_3\text{O}_{7-\delta}$ -type compounds. *Journal of Raman Spectroscopy* **27**(3-4) (1996), 333-342.
- [13] Li Y.B., Shelley C., Cohen L.F., Caplin A.D., Strading R.A., Kula W., Sobolewski R. and MacManus-Driscoll J.L. Raman studies of laser written patterns in $\text{YBa}_2\text{Cu}_3\text{O}_x$ films. *Journal of Applied Physics* **80**(5) (1996), 2929-2934.
- [14] Venkataraman K., Baurceanu R. and Maroni V.A. Characterization of $\text{MBA}_2\text{Cu}_3\text{O}_{7-x}$ thin films by Raman microspectroscopy. *Applied Spectroscopy* **59**(5) (2005), 639-649.